ESO Science Archive Facility - Phase 3 Data Release Description
ESO public survey programme LEGA-C - Large Early Galaxy Astrophysics Census, Data Release DR2
provided by Arjen van der Wel, submitted between 2018-03-29 and 2018-06-13, published on 2018-06-21

The Large Early Galaxy Astrophysics Census (LEGA-C) – DATA RELEASE II

Abstract

We present the second data release of the Large Early Galaxy Astrophysics Census (LEGA-C), an ESO 130−night public spectroscopic survey conducted with VIMOS on the Very Large Telescope. We release 1989 spectra with typical continuum S/N ≃ 20 Å of galaxies at 0.6 < z < 1.0, each observed for ∼ 20 hours and fully reduced with a custom-build pipeline. The survey covers the 1.6 square degrees of the UltraVISTA survey within the in the COSMOS field (R.A. = 10h00; Dec. = +2 deg). The VIMOS high-resolution red grating is used in combination with the GG475 order separation filter, which results in a typical wavelength range of ∼ 6300Å – 8800Å at a resolution of R = 2500 and a dispersion of 0.6Å per pixel.

LEGA-C's unique combination of sample size and depth enables for the first time to map the stellar content at large look-back time (8 Gigayears), across galaxies of different types and star-formation activity. Core science goals are, among others, to chart the star formation histories of galaxies, quenching of star formation, evolution of galaxy kinematics and other scaling relations. Observations started in December 2014 and were completed by March 2018. The full survey will comprise > 4000 spectra of > 3000 sources.

In this release, we provide the data resulting from our first two years of observations (programs 194.A-2005(A) to 194.A-2005(N)), totaling 1988 galaxy spectra of 1922 unique galaxies. We also release a catalog with spectroscopic redshifts, emission line fluxes, Lick/IDS indices, and spatially integrated stellar and gas velocity RMSs (line widths).

Full details about the survey design, sample selection, observing strategy, data reduction, and science goals can be also found in two survey papers:

"THE VLT LEGA-C SPECTROSCOPIC SURVEY: THE PHYSICS OF GALAXIES AT A LOOKBACK TIME OF 7 GYR": A. van der Wel , K. Noeske, R. Bezanson, C. Pacifici, A. Gallazzi, et al. 2016, ApJS, 223, 29

Hereafter referred to as W16;

"THE LARGE EARLY GALAXY ASTROPHYSICS CENSUS (LEGA-C) DATA RELEASE II: DYNAMICAL AND STELLAR POPULATION PROPERTIES OF Z<1 GALAXIES IN THE COSMOS FIELD." Straatman et al., submitted.

Overview of Observations

We release data of masks 1 through 15 out of 32. The masks were observed during the ESO observing periods 94 to 98, from December 2014 to January 2017. Due to visibility constraints, most of these nights were fractional allocations to LEGA-C. Observations were conducted in visitor mode, during dark time periods, and in good weather conditions (seeing <1.3"). During sufficiently long time windows when these conditions were not achieved, the telescope was handed back to ESO staff to be used for Service Mode programs.

Every mask was observed during 15-35 Observing Blocks (OBs) of four 450 - 900 second long exposures, depending on observing conditions. A mask was completed after ∼ 20 hours depending on the conditions. No dithering was applied to avoid severe efficiency costs. This is additionally justifiable by the sufficiently low amplitude of fringing found in the spectra. Dithering would sacrifice 16% − 30% in depth, equivalent to 6 − 10 hours of exposure time.

Calibrations were obtained in a non-standard manner, again to avoid a severe penalty in survey efficiency. Initially, arcs and screen flats were not taken directly after each science OB, but at the end of the (partial) night and at the average of the rotator angles of each OB observed that night.

However, subsequent analysis of the full calibration dataset showed that proximity in time to the science exposures is more relevant to minimize the effects of flexure and hysteresis than the rotator angle, so our strategy was changed to taking calibration exposures every two to two and a half hours between science OBs. For short partial nights, i.e., less than two hours of allocated time, we only obtained calibration data once before or after observing the science OBs. We do not use spectrophotometric standards to flux-calibrate the spectra, but rather use the rich and well-calibrated photometric spectral energy distributions from the UltraVISTA catalog to derive the calibration.

Release Content

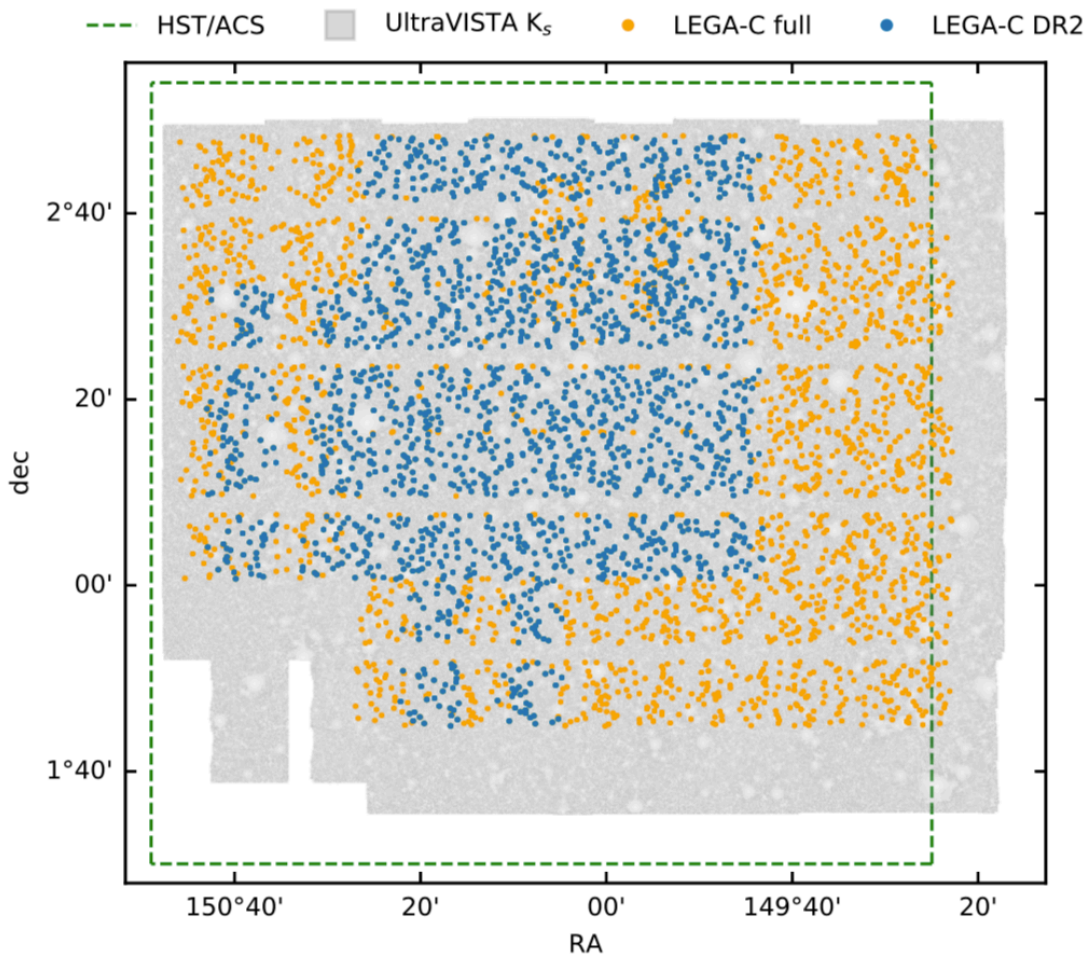

The position and extent on the sky for sources in DR2 as well as the mask numbers can easily be inferred from the target coordinates and mask numbers given in the catalog ("legac_DR2.fits". The above figure shows a footprint of the COSMOS field, with targeted LEGA-C sources shown in orange. Those included in DR2 are shown in blue. The green frame indicates the dimensions of the COSMOS field as observed with HST/ACS and the gray image in the background is the Ks-band image from UltraVISTA.

The primary targets are chosen from a K–band magnitude selected parent sample of ~ 10,000 galaxies with photometric redshifts z = 0.6 – 1 drawn from the UltraVISTA catalog (Muzzin, A., Marchesini, D., Stefanon, M., et al. 2013a, ApJS, 206, 8), which overlaps for the most part with the already extensively photometrically covered COSMOS field. The K–band limit ranges from K < 21.08 at z = 0.6 to K < 20.36 at z = 1.0, overall this results in a sample with a stellar mass limit of the order of ~ 10^10 solar mass. Targets for the VIMOS masks were inserted in order of K–band magnitude (brightest first) while avoiding slit collisions and independent of environment. Any

remaining space in the masks was used to include 'fillers'. Ordered by priority these are 1) galaxies at z > 1 and brighter than K = 20.4; 2) galaxies at z < 1 and fainter than our K-band magnitude limit. Both of these subsamples are also ranked by K–band magnitude when designing the masks. The sample to be released in DR2 consists of 1550 primary targets and 438 'fillers'.

DR2 comprises 1988 individual 1-D spectra of 1922 unique sources (some were included in more than one mask) as well as a survey catalog with entries for each spectrum. The total data volume is 205 Mb.

• Release Notes

The spectra have a topocentric reference coordinate system, with wavelengths measured in dry air.

Data Reduction and Calibration

The raw frames were obtained from the ESO archive and processed through the recommended ESO tools at the time of observation: Reflex versions 2.7-2.8.5 (Freudling, W., Romaniello, M., Bramich, D. M., et al. 2013, A&A, 559, A96) with the VIMOS pipeline package versions 2.9.15-3.1.9.

- We employ a custom pipeline to further analyze the Reflex data products. This is motivated by the need to remove bleeding of bright skylines between slits, correct for small misalignments between science and calibration exposures due to instrument flexure, the need for accurate sky-subtraction for extended objects, and optimal S/N–weighted extraction of spectra from the different OBs. An initial version of this custom pipeline was used for Data Release I and described in W16. For Data Release II a number of refinements are added and all spectra, including those from Data Release I, were processed or re-processed using the latest version of the pipeline. The custom pipeline performs the following steps:

    - Variance spectra are calculated from the (background + object) flux and the read noise on a pixel-by-pixel basis.

    - Slit definitions, i.e., the locations of sources, are verified and if necessary adjusted, with a margin at the top and bottom of the slit against bleeding of skyline flux from neighboring slits.

    - The location and spatial extent (FWHM) of the sources are measured by fitting a Gaussian in the spatial direction after summing along ~ 800 pixels in the wavelength region between 7120 Å and 7600 Å, which is free of bright atmospheric emission lines. The location of the source is then traced along the entire wavelength range in bins of 100 pixels through a weighted fit using the variance spectrum. If there is insufficient flux to do this, the location over the entire wavelength range is assumed to be the expected location from the mask design.

    - We then build a galaxy+sky model for each wavelength pixel. This includes the Gaussian with a fixed location and FWHM as defined above, but with the amplitude as a free parameter, and with a constant (sky) flux level as a second free parameter. To account for areas with high sky levels or large sky level gradients in the wavelength direction, e.g., near the edges of skylines, a first-order term is added to allow for a sloping background in the spatial direction.

    - Telluric absorption features are corrected by dividing by a normalized blue star spectrum. Each mask contains a blue star, selected to have an SDSS color (g - r) < 0.5, corresponding to spectral type F or earlier. We only applied corrections in wavelength regions with significant telluric absorption (6865 - 6960 Å, 7160 - 7330 Å,

7580 - 7710 Å, 8070 - 8400 Å, 8900 - 9200 Å), so that stellar features outside those windows do not lead to spurious features in the galaxy spectra.

- Spectra from individual OBs are aligned and coadded after weighting by the S/N as measured between 7120 Å and 7600 Å.

- Many galaxies have faint, extended wings in our deep spectra that are not accurately captured with the Gaussian extraction kernel we use to model the sky+object in the individual OBs. We therefore revisit the sky sub- traction in the coadded 2D spectra, which have a much higher S/N than the single OB spectra and allow for a better assessment of the extended light. Summing over all wavelength pixels between 7120 Å and 7600 Å we fit a Moffat profile to the flux of the source. Keeping the shape of the Moffat profile fixed we then create a new model for sky+object for each column of pixels with the same wavelength, where we vary only the amplitude and sky background (constant+slope). Third- order polynomials are then fit to the sky parameters to create a smooth master sky model which is then subtracted from the 2D spectrum and propagated into the 1D extracted spectrum by using the Moffat profile as the extraction kernel.

- Secondary objects are identified automatically in the coadded spectra by searching for significant peaks of continuum flux. If a spectrum contains a secondary source, the sky background in the previous steps will have been overestimated, so we perform a second sky subtraction after fitting two Moffat components to the coadded spectrum.

- Emission lines trace the kinematics and spatial structure of gas, which are often different from that of the stellar continuum. For these reasons the Moffat profile that is used to characterize the spatial structure of the continuum light of a galaxy does not accurately reflect the light distribution of emission lines. As such, the sky subtraction near emission lines can be inaccurate. We identify emission lines by searching for significant peaks in smoothed 1D spectra and redo the sky+object Moffat modeling while leaving the spatial location as an additional free parameter across a 40-pixel region around the central wavelength of the emission line.

- Spectra are flux calibrated using the photometric SEDs from UltraVISTA. Best-fit spectral templates for these were obtained with FAST after updating with the spectroscopic redshifts and fit with a 5th order polynomial across the wavelength range of the LEGA-C spectra. Another 5th order polynomial is fit to the LEGA-C spectra and the ratio between the two is used to scale the LEGA-C spectra in a wavelength dependent way. We note that the flux calibration compensates for slit losses assuming that the spectrum is the same in shape across the galaxy, but does not account for wavelength-dependent spatial gradients along the slit. We also note that in this way emission line fluxes receive the same correction, implicitly assuming slit losses are the same for the continuum and the lines.

Some sources were observed more than once over different masks. They appear as different entries in the catalog and can be distinguished by their unique identifier, which is a combination of the mask number and the ID ([mask number]_[source ID]).

Intergalactic extinction has indirectly been taken into account by using the UltraVISTA photometry.

Catalog

Values in the catalog were derived after fitting each spectrum with two template sets using the Penalized Pixel-Fitting (pPXF) code (Cappellari, M., & Emsellem, E. 2004, PASP, 116, 138) with the updated Python routines (Cappellari, M. 2017, MNRAS, 466, 798). These consisted of a collection of high resolution (R = 10 000) single stellar population templates (Conroy et al., in prep.), to

fit the continuum, as well as a collection of possible emission lines ([NeV], [NeVI], H10, H9, H8, Hδ, Hγ, Hβ, [OII]3726,3729, [NeIII], [SII]6717,6731, [OIII]5007, [OIII]4959, [OIII]4363, [NI]), to fit the ionized gas emission. The fluxes were allowed to vary independently, but the linewidths were constrained to be the same (see also W16, Bezanson, R., van der Wel, A., Pacifici, C., et al. 2018, ArXiv e-prints, arXiv:1804.02402 , Bezanson et al. in prep).. The emission line fluxes in the catalog were derived from integrating the best-fit emission line set at locations where an emission line was found. Equivalent widths were derived by dividing the line flux by the local best-fit continuum, here defined as the average of the continuum in a 200 Å wide region centered on the line. Lick/IDS indices as described in Worthey, G., Faber, S. M., Gonzalez, J. J., & Burstein, D. 1994, ApJS, 94, 687 and Worthey, G., & Ottaviani, D. L. 1997, ApJS, 111, 377, including the higher order Balmer lines, $H\gamma_A$ and $H\delta_A$, and the narrow definition of the 4000 Å break ($D4000_n$), were derived following the analysis in Gallazzi, A., Bell, E. F., Zibetti, S., Brinchmann, J., & Kelson, D. D. 2014, ApJ, 788, 72 after subtracting the best-fit emission line model. Missing values, (due to, e.g., no coverage) are set to NaN in the catalog. For the Lick/IDS indices, in case of sufficient coverage, but only with <80% good pixels in the central or pseudo-continuum bandpasses, the values are still included in the catalog, but the uncertainty is set to NaN.

The catalog further contains a completeness correction factor accounting for the target selection procedure, which can be used to translate the LEGA-C sample into a volume limited sample. Finally there are three different S/N estimates included: 1) the overall median S/N per pixel of the spectra, 2) the S/N measured at rest-frame 4000 Å, and 3) the S/N measured at observed-frame 8030 Å.

Data Quality

- Reduction and quality control: the output of the custom-made pipeline was visually verified on an OB-by-OB and object-by-object basis. Any problems with the slit definition, tracing, and sky subtraction were identified and, if appropriate, the pipeline was rerun. The combined 1D and 2D spectra were verified on an object-by-object basis as well.

- Formal uncertainties on released quantities were derived from the variance spectra. In general, we find that those agree well with the noise level seen in the spectra themselves. Yet they do not take into account additional sources of error, such as variations in seeing or imperfect sky subtraction. The formal uncertainties were verified using the duplicate spectra. We derived factors of 1.25x to 3x larger scatter between duplicate observations and based on this applied multiplicative factors to the uncertainties released in the catalog. The uncertainties in this data release are thus final, corrected uncertainties.

- A small number of spectra were rejected on the basis of fundamental flaws (e.g. imperfect sky subtraction, a bad wavelength solution, mismatch between OBs, absence of light because of vignetting) in the observed spectra or data reduction process and received a flag $f_{spec} = 1$. For a few galaxies we could not measure the redshift: $f_z = 1$ (due to e.g., vignetting or low S/N.) We note that redshift information is unambiguous for our spectra due to the number of features at high S/N, so that there is no need for a quality flag for the redshift measurement as is common practice for redshift surveys. Finally, in a few cases the pPXF fit is flawed: ($f_{pPXF} = 1$). The spectroscopic sample of primary survey targets that can be used for scientific purposes ($f_{use} = 1$) combines these flags:

  $f_{primary} = 1$ and $f_{spec} = 0$ and $f_z = 0$ and $f_{pPXF} = 0$

  1442 of 1550 primaries (with $f_{primary}=1$) have $f_{use} = 1$.

- In addition to the use flag we include an interpretation flag (f_{int}), which is a separate flag from f_{use} indicating any of the value added quantities may need extra attention, for example in the case of an unresolved merging system. Since the quality of the spectra in these cases can still be good, f_{int} is a separate flag from f_{use} and some sources with $f_{use}=1$ may also have $f_{int}=1$.

Known issues

- Object alignment within the slits: During the observations, some acquisition images taken for the mask alignment showed slight offsets where the galaxies were not perfectly centered within the slits, but offset in dispersion direction (detector y-coordinate). Despite carefully repeated efforts, a perfect alignment was not always possible for all 4 mask quadrants that have to be simultaneously aligned. A post hoc extensive analysis of alignment images from three masks revealed a pattern where the alignment of the objects varies relatively smoothly across VIMOS' field of view. This systematic suggests that the source of this issue is not the accuracy of coordinates in our target catalog, but in the accuracy of the optical model in the VIMOS mask design software. The effect amounts to average object offsets in dispersion direction of: -0.14 pixels in quadrant 1, +0.23 pixels in quadrant 2, +0.08 pixels in quadrant 3 and -0.35 pixels in quadrant 4, with offsets measured with respect to the positive detector y coordinate (dispersion direction). The standard deviation of object misalignments in detector y-coordinate was 0.8 pixels for all quadrants.
  This result means that for some galaxies, their PSF is not fully contained within the slit, possibly leading to fractional flux losses that will depend strongly on the galaxy's morphology and light concentration. The resulting slit losses range from 10% to 40%. Since absolute flux calibrations are obtained from broadband photometry (see "Data Reduction and Calibration"), such losses are mostly compensated for in the calibrated spectra. However, the accuracy of the flux calibration, typically 5% for individual galaxies, may be affected for some sample targets. Because galaxies have radial gradients in their spectral energy distribution, both the limited slit width capturing only a part of the galaxy, as well as slight slit misalignments, inevitably introduce wavelength-dependent calibration imperfections in a spectroscopic study.

Previous Releases

Data Release I.

This second data release differs from the first data release as follows:

- The sample size increased from 892 to 1988 galaxies.
- The catalog has been expanded to include velocity dispersion values and absorption and emission line measurements.
- The sky subtraction algorithm was improved in three ways:
  1. The spatial light profiles are modeled with a Moffat function instead of a Gaussian, improving the characterization of the faint wings and avoiding over subtraction of the sky level;
  2. secondary objects in the slit are treated as such;
  3. emission lines are no longer assumed to spatially coincide with the stellar continuum, avoiding the effects of spatial offsets of gas and stars, as well as the effect of Doppler shifts. For more details, see the ``Data Reduction and Calibration" Section and the data release paper (Straatman et al., submitted).

• Data Format

Files Types

- One catalog file: legac_DR2.fits, a one-extension FITS binary table, with columns described in the next subsections.
- 1989 1-dimensional spectra, containing one galaxy spectrum each, named:
- "legac_M[mask number]_[legac target ID]_v1.0.fits"

Spectra

The 1-d spectra files hold the spectrum in their sole binary table extensions, in four columns:

1. Wavelength, label="WAVE", unit Å, format 4-byte FLOAT
2. Flux, label "FLUX", unit 10^{19} erg s^{-1} cm^{-2} $Å^{-1}$, format 4-byte FLOAT
3. Flux error, label "ERR", unit 10^{19} erg s^{-1} cm^{-2} $Å^{-1}$, format 4-byte FLOAT
4. Quality flag, label "QUAL" (no unit), format 2-byte INTEGER

Note on flux error and quality flag: some elements in the "error" column are set to zero. This does however NOT indicate a very small error, but rather means that this element should be excluded from further analysis. Such elements show a large second derivative in the spectrum, too large to be explained by spectra features or random noise, which typically indicates the presence of a systematic imperfection in the sky subtraction at that location. For such elements, the quality flag is set to 1.

Catalogue Columns

The catalog "legac_DR1.fits" contains for each spectrum the target galaxy's LEGA-C object ID, the number of the mask containing the object, RA and DEC, spectroscopic redshifts, velocity RMSs, Lick/IDS indices, emission line fluxes and equivalent widths, and quality flags. These values are given in the file's sole binary table extension, with columns as follows:

Column	**Label**	**Unit**	**Format**
Target ID	OBJECT	na	4 byte long integer
Mask number + target ID	SPECT_ID	na	Ascii string
Right ascension (J2000.0)	RAJ2000	Degrees	8-byte double precision float
Declination (J2000.0)	DECJ2000	Degrees	8-byte double precision float
Redshift	Z	na	4-byte float
Filename of 1-d spectrum	Filename	na	Ascii string
Observed stellar velocity dispersion	SIGMA_STARS_PRIME	km s^{-1}	4-byte single precision float
Observed stellar velocity dispersion error	SIGMA_STARS_PRIME _err	km s^{-1}	4-byte single precision float
Observed gas velocity dispersion	SIGMA_GAS_PRIME	km s^{-1}	4-byte single precision float
Observed gas velocity dispersion error	SIGMA_GAS_PRIME _err	km s^{-1}	4-byte single precision float
LICK CN1 index	LICK_CN1	Å	4-byte single precision float
LICK CN1 index error	LICK_CN1_err	Å	4-byte single precision float
LICK CN2 index	LICK_CN2	Å	4-byte single precision float
LICK CN2 index error	LICK_CN2_err	Å	4-byte single precision float
LICK CA4227 index	LICK_CA4227	Å	4-byte single precision float
LICK CA4227 index error	LICK_CA4227_err	Å	4-byte single precision float
LICK G4300 index	LICK_G4300	Å	4-byte single precision float
LICK G4300 index error	LICK_G4300_err	Å	4-byte single precision float
LICK FE4383 index	LICK_FE4383	Å	4-byte single precision float

LICK FE4383 index error	LICK_FE4383_err	Å	4-byte single precision float
LICK CA4455 index	LICK_CA4455	Å	4-byte single precision float
LICK CA4455 index error	LICK_CA4455_err	Å	4-byte single precision float
LICK FE4531 index	LICK_FE4531	Å	4-byte single precision float
LICK FE4531 index error	LICK_FE4531_err	Å	4-byte single precision float
LICK C4668 index	LICK_C4668	Å	4-byte single precision float
LICK C4668 index error	LICK_C4668_err	Å	4-byte single precision float
LICK HB index	LICK_HB	Å	4-byte single precision float
LICK HB index error	LICK_HB_err	Å	4-byte single precision float
LICK HD_A index	LICK_HD_A	Å	4-byte single precision float
LICK HD_A index error	LICK_HD_A_err	Å	4-byte single precision float
LICK HG_A index	LICK_HG_A	Å	4-byte single precision float
LICK HG_A index error	LICK_HG_A_err	Å	4-byte single precision float
LICK HD_F index	LICK_HD_F	Å	4-byte single precision float
LICK HD_F index error	LICK_HD_F_err	Å	4-byte single precision float
LICK HG_F index	LICK_HG_F	Å	4-byte single precision float
LICK HG_F index error	LICK_HG_F_err	Å	4-byte single precision float
LICK D4000_N index	LICK_D4000_N	Å	4-byte single precision float
LICK D4000_N index error	LICK_D4000_N_err	Å	4-byte single precision float
Hδ emission line flux	Hd_flux	10^{19} erg s^{-1} cm^{-2} $Å^{-1}$	4-byte single precision float
Hδ emission line flux error	Hd_flux_err	10^{19} erg s^{-1} cm^{-2} $Å^{-1}$	4-byte single precision float
Hδ emission line EW	Hd_EW	Å	4-byte single precision float
Hδ emission line EWerror	Hd_EW_err	Å	4-byte single precision float
Hγ emission line flux	Hg_flux	10^{19} erg s^{-1} cm^{-2} $Å^{-1}$	4-byte single precision float
Hγ emission line flux error	Hg_flux_err	10^{19} erg s^{-1} cm^{-2} $Å^{-1}$	4-byte single precision float
Hγ emission line EW	Hg_EW	Å	4-byte single precision float
Hγ emission line EWerror	Hg_EW_err	Å	4-byte single precision float
Hβ emission line flux	Hb_flux	10^{19} erg s^{-1} cm^{-2} $Å^{-1}$	4-byte single precision float
Hβ emission line flux error	Hb_flux_err	10^{19} erg s^{-1} cm^{-2} $Å^{-1}$	4-byte single precision float
Hβ emission line EW	Hb_EW	Å	4-byte single precision float
Hβ emission line EWerror	Hb_EW_err	Å	4-byte single precision float
[OII]3727 emission line flux	OII_3727_flux	10^{19} erg s^{-1} cm^{-2} $Å^{-1}$	4-byte single precision float

[OII]3727 emission line flux error	OII_3727_err	10^{19} erg s^{-1} cm^{-2} $Å^{-1}$	4-byte single precision float
[OII]3727 emission line EW	OII_3727_EW	Å	4-byte single precision float
[OII]3727 emission line EWerror	OII_3727_EW_err	Å	4-byte single precision float
[OIII]4959 emission line flux	OIII_4959_flux	10^{19} erg s^{-1} cm^{-2} $Å^{-1}$	4-byte single precision float
[OIII]4959 emission line flux error	OIII_4959_err	10^{19} erg s^{-1} cm^{-2} $Å^{-1}$	4-byte single precision float
[OIII]4959 emission line EW	OIII_4959_EW	Å	4-byte single precision float
[OIII]4959 emission line EWerror	OIII_4959_EW_err	Å	4-byte single precision float
[OIII]5007 emission line flux	OIII_5007_flux	10^{19} erg s^{-1} cm^{-2} $Å^{-1}$	4-byte single precision float
[OIII]5007 emission line flux error	OIII_5007_err	10^{19} erg s^{-1} cm^{-2} $Å^{-1}$	4-byte single precision float
[OIII]5007 emission line EW	OIII_5007_EW	Å	4-byte single precision float
[OIII]5007 emission line EWerror	OIII_5007_EW_err	Å	4-byte single precision float
ppxf flag	f_ppxf	Na	1-byte unsigned byte
Redshift flag	f_z	Na	1-byte unsigned byte
Spectroscopic flag	f_spec	Na	1-byte unsigned byte
Primary target flag	f_primary	Na	1-byte unsigned byte
Use flag	f_use	Na	1-byte unsigned byte
Interpretation flag	f_int	Na	1-byte unsigned byte
Completeness correction factor	Tcor	$pixel^{-1}$	4-byte single precision float
Overall median S/N per pixel	SN	$pixel^{-1}$	4-byte single precision float
S/N at rest-frame 4000 Å	SN_RF_4000	$pixel^{-1}$	4-byte single precision float
S/N at observed-frame 8030 Å	SN_OBS_8030	$pixel^{-1}$	4-byte single precision float

• Acknowledgements

Please use the following statement in your articles when using these data:

"Based on data products from observations made with ESO Telescopes at the La Silla Paranal Observatory under program ID 194.AF2005(A-N)."